Direct femtosecond mapping of trajectories in a chemical reaction

A. Mokhtari, P. Cong, J. L. Herek & A. H. Zewail

Arthur Amos Noyes Laboratory of Chemical Physics,
California Institute of Technology, Pasadena, California 91125, USA

In chemical reactions, the dynamics of the transition from reagents to products can be described by the trajectories of particles (or rigorously, of quantum mechanical wave packets) moving on a potential-energy surface. Here we use femtosecond pulsed laser techniques to follow directly the evolution in space and time of such trajectories during the breakage of a chemical bond in the dissociation of sodium iodide. The bond breakage can be described in terms of the time evolution of a single reaction coordinate, the internuclear separation. As the velocities of the separating fragments are typically of the order of a kilometre per second, a time resolution of a few tens of femtoseconds is required[1,2] to view the motions on a molecular distance scale of less than an ångstrom. The resolution obtained here permits the direct visualization of the wave packet's motion and provides snapshots of the trajectories along the reaction coordinate.

The potential-energy surface (PES) for the NaI reaction (Fig. 1) involves two channels; one describes the covalent character of the bond (Na + I) and the other the ionic character ($Na^+ + I^-$). The two potential curves intersect at an internuclear separation R of 7 Å. When NaI is promoted with a femtosecond (pump) pulse to the covalent curve at $R \simeq 2.7$ Å, the wavefunction (or, more accurately, the wave packet) moves towards the ionic curve and then returns with a period determined by the shape of the PES and the total energy in the bond[3,4]. Using a femtosecond probe pulse, we can monitor the oscillation of this activated complex[5], $[Na\cdots I]^{\ddagger}$ as it decays, on a picosecond timescale, to give Na and I (Fig. 1 inset).

Figure 2 shows trajectories in the R–t domain. Both classical newtonian mechanics[3,4,6] and quantum mechanics[7] calculations have been performed; here we consider the former approach to illustrate the methodology. As shown in Fig. 2, the wave packet changes direction as R and t change, starting from the initial time zero at $R \simeq 2.7$ Å. After half a period the packet has reached the ionic turning point, and after a complete period it has returned to the covalent turning point. At or near the ionic–covalent crossing, the packet splits; some continues to move in the direction of increasing R, becoming Na and I, and the rest remains as $[Na\cdots I]^{\ddagger}$, oscillating between the covalent and ionic points. (See also Fig. 1.)

To observe the motion of the trajectories, a window in $R(t)$ must be opened with sufficient distance resolution ΔR to allow us to view the directionality of the packet at different times. If the window is stepped continuously along R, then we can map out the motion and characteristics of the PES. For a given resolution, the temporal motion represents a 'snapshot' of the

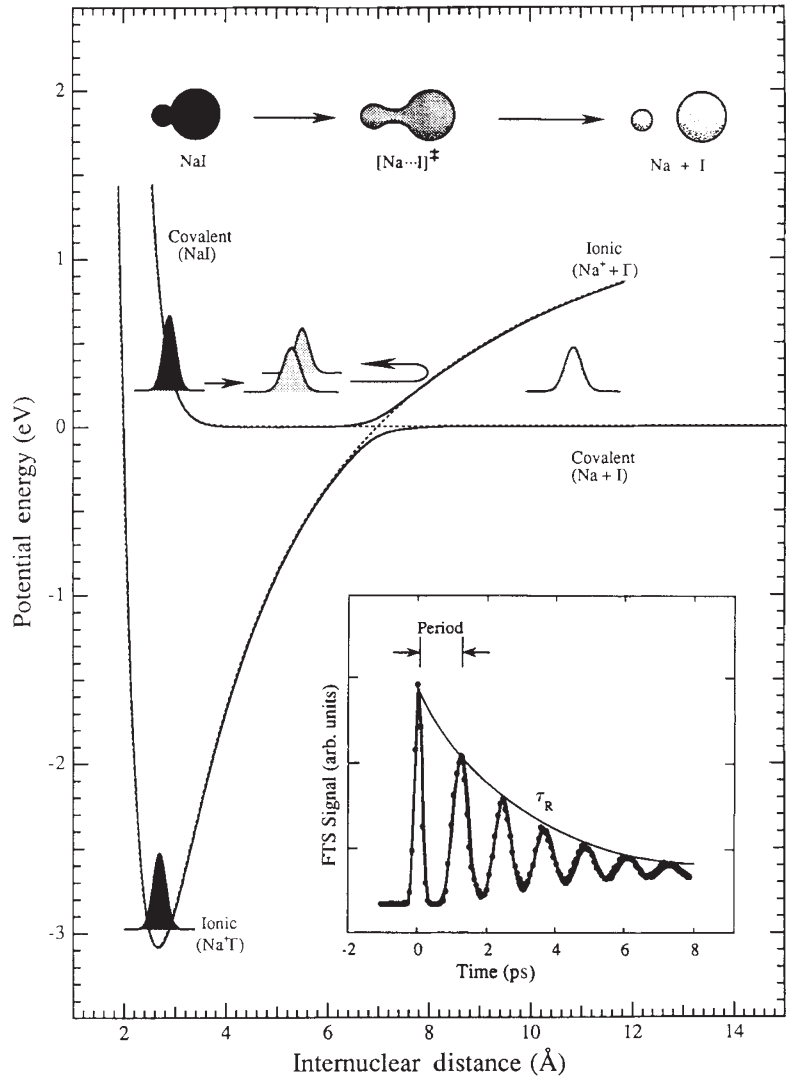

FIG. 1 Schematic diagram of the wave-packet motion in the dissociation reaction of NaI. The femtosecond pump pulse 'transfers' the ground-state wavefunction to the adiabatic potential formed by the avoided crossing of the ionic and covalent curves. The wave packet then moves back and forth, leaking a little (~10%) to Na + I every time it approaches the crossing region. The probe femtosecond pulse monitors this oscillatory motion and the decay (τ_R), as shown in the insert.

PES at this particular R. For example, a window at $R = 3$ Å will give the snapshot shown at the bottom of Fig. 2, which is basically the oscillatory motion displayed in Fig. 1. On the other hand, if a snapshot is taken at $R = 4.5$ Å, the oscillatory motion displays a splitting because at this distance the packet is going in and out of the probing ΔR window. At longer R the splitting increases in time, because the distance the trajectory travels is longer. The observation of such splittings would indicate two important points. First, it would mean that the window opened in R is sufficiently narrow[8] to resolve the nuclear motion in and out of that region of the PES. Second, the splitting gives a time (at each R) that is directly related to the clocking time, defined[9] by the distance travelled from time zero to the probing point on the PES.

The experiments required pump and probe pulses tunable between 310 nm and 390 nm, and between 590 nm and 700 nm, respectively. Briefly, a colliding-pulse mode-locked ring dye laser, generating 50-fs pulses around 620 nm, was amplified in a Nd:YAG-pumped four-stage dye amplifier. The output pulses from the amplifier were temporally recompressed in a sequence of four high-refractive-index glass prisms. The tunability on the probe arm was achieved by generating a white-light continuum, and the same procedure was used on the pump arm, except that the light was further amplified in a flowing cell of the appropriate laser dye (pumped by 532-nm pulses from the Nd:YAG source). We used nonlinear doubling and mixing techniques for conversion to ultraviolet. The pump and probe beams were focused in a NaI reaction chamber and the laser-induced fluorescence was collected perpendicular to the propagation direction of the pump and probe beams. The time delay between the pump and probe was controlled by a high-precision Michelson interferometer and the experiments were controlled by a computer. The range of R probed is shown in Fig. 3.

Figure 4 shows our experimental observations for the NaI reaction. The packet was prepared by a femtosecond pulse at a wavelength λ_1. To probe at different R, we used another femtosecond pulse of different wavelength λ_2. For a given total energy in the bond, determined by λ_1, both the time and the λ_2 can be changed systematically to obtain the snapshots at different R. In Fig. 4, we show three snapshots for $\lambda_1 = 391$ nm as examples of the many snapshots we took. The evolution of the splitting as λ_2 decreases (that is, as R increases) is evident. The splitting at $\lambda_2 = 620$ nm, for example, is 350 fs. This gives a clocking time for the packet to reach the window on the PES of 175 fs. The actual distance being probed is 5.6 Å, as determined by the velocity of recoil. The window resolution is very appropriate for the dynamical motion of chemical reactions: the temporal splitting observed gives an experimental $\Delta R \simeq 0.5$ Å on the PES. The potential for these types of reactions is quite flat at intermediate R (see Fig. 1), and therefore even better resolution may be achieved in other reactions.

For NaI dissociation, the probe at λ_2 excites the wave packet to an upper surface corresponding to the $Na^* + I$ channel. The relationship between λ_2 and R is direct if this upper surface is flat at longer R, as discussed in refs 3 and 4. We have determined that there is a well (depth $\simeq 1{,}500\ cm^{-1}$, which is deeper than the well reported in ref. 10) in the region probed, which allows us to look at the different regions of the PES shown in Fig. 3. For a given λ_2, we can determine characteristics of the covalent curve by changing λ_1—direct clocking on the lower surface.

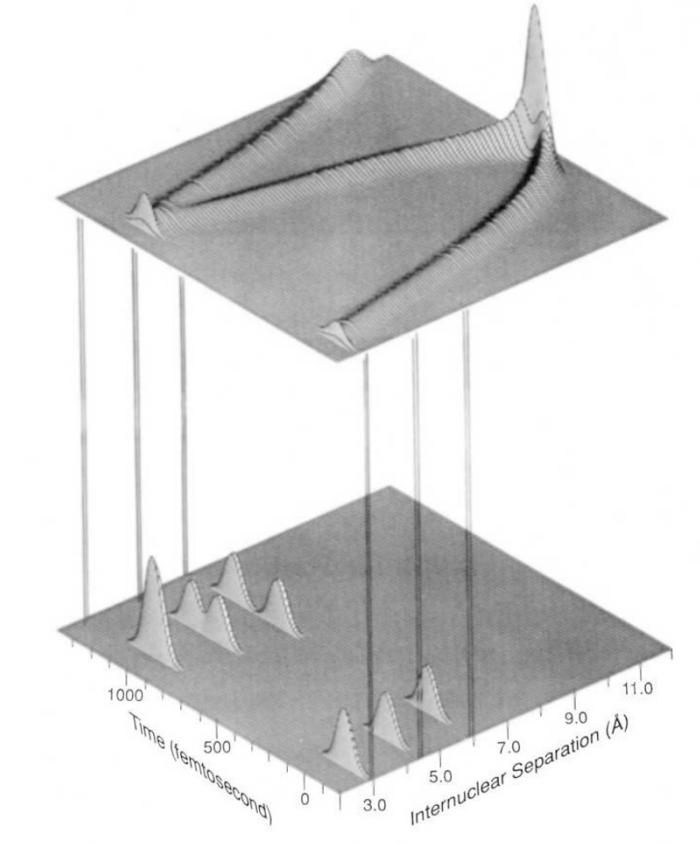

FIG. 2 Classical mechanics simulation of the wave-packet motion with a femtosecond pump pulse at 320 nm. The upper plot shows the wave-packet motion in the two-dimensional space of time and internuclear separation. For simplicity, we do not show the leakage at the crossing point. The lower plot shows the snapshots of the wave-packet motion at different internuclear separations. Note the evolution of the splitting.

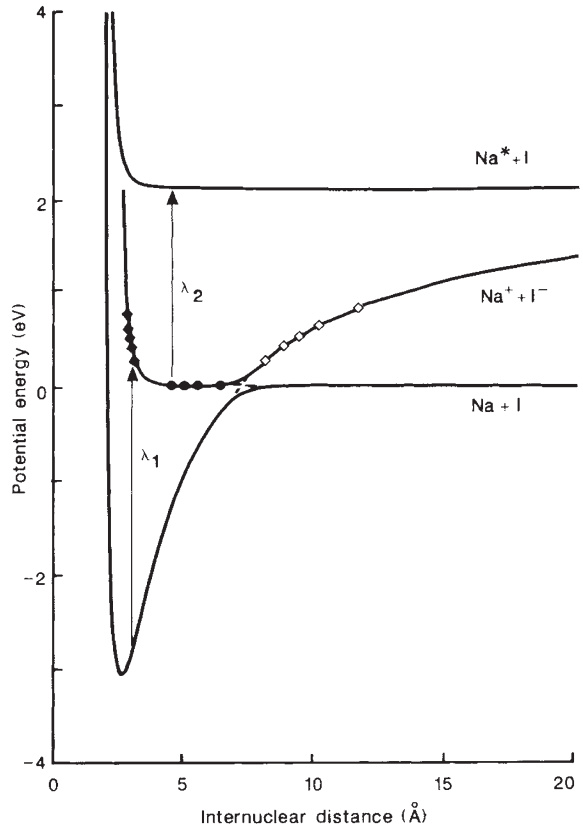

FIG. 3 The range of internuclear distances probed in the experiments. The filled diamonds represent the range that can be reached by pump (λ_1) pulses, the filled circles show the internuclear separations accessed by the probe (λ_2) pulses, and the open diamonds show the points that can be obtained from the oscillation periods. The potentials drawn are taken from ref. 2. We plan to use the snapshots results to deduce more accurate potentials[8].

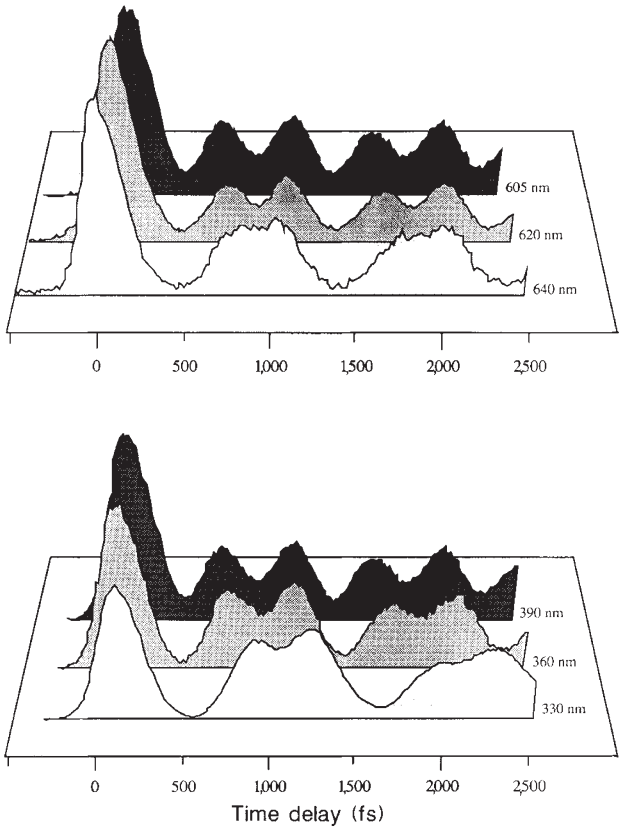

FIG. 4 Experimental femtosecond snapshots of NaI reaction. The upper panel shows the snapshots taken at different probe wavelengths for a wave packet prepared by exciting the NaI molecule at 391 nm (fixed total energy in the bond). The lower panel shows the snapshots taken at a constant λ_2 of 605 nm, while varying the original position (R_0) of the wave packet (different total energies).

Changing the total energy $E_1 = \frac{1}{2}\mu v^2$ and repeating the probing gives the motion on different parts of the PES. The reduced mass μ is constant and by changing λ_1 or E_1 one changes the velocity of recoil v. As E_1 is decreased, we expect the velocity to decrease and the distance travelled by the wave packet, to a given R, to also decrease. Depending on the PES, these two effects determine whether or not the splitting will increase or decrease with E_1. Figure 4 shows three snapshots at different λ_1. We observe an increase in the splitting as E_1 is lowered. We also observe a decrease in the period. The latter is consistent with the potential 'narrowing' in R at lower E_1. The former indicates that the covalent side of the potential is very repulsive at short R and is dominated by velocity (not distance) effects, as shown in Fig. 3.

Theoretically, the use of classical mechanics may be sufficient to describe the global motion on the PES. In fact, the results of our experiments and the classical mechanics calculations in Fig. 2 are in agreement. We have, however, done quantum mechanical calculations to justify the agreement between the classical trajectory $R(t)$ and the quantum mechanical expectation value $\langle R(t)\rangle$ (ref. 11). Quantum mechanical calculations at three pump wavelengths, 310 nm, 350 nm and 390 nm indicate that the results agree with those for classical mechanics. The only discrepancy occurs close to the turning point on the steep repulsive branch—this arises because the average position of the wave packet does not reach the classical turning point. Rigorous quantum mechanical calculations of the wave-packet propagation[12] have shown evidence for the splitting; the interpretation did not address the clocking and mapping-of-trajectories aspect of the problem. For NaI, the reduced mass is relatively heavy and the spread of the wave packet, a quantum mechanical feature, is only expected at longer times[11]. More theoretical and experimental work is in progress.

The results reported here show that the motion of the nuclear wave packet during the breaking of the NaI bond can be probed with an experimental resolution of ~0.5 Å of internuclear separation. The position of the probing 'window' can be varied to map the trajectories $R(t)$. The packet is observed in real time for both contraction and extension of the NaI chemical bond as it passes through the window in both directions. The range of internuclear distances probed—up to 6.5 Å on the covalent and 12 Å on the ionic curves—shows the ability of the method to yield direct information on the potential-energy curves at large internuclear separations. This development promises a wide range of applications to other reactions, including those characterized by multidimensional potential-energy surfaces. □

Received 12 October; accepted 22 October 1990.

1. Zewail, A. H. *Science* **242,** 1645–1653 (1988).
2. Khundkar, L. R. & Zewail, A. H. *A. Rev. phys. Chem.* **41,** 15–40 (1990).
3. Rose, T. S., Rosker, M. J. & Zewail, A. H. *J. chem. Phys.* **88,** 6672 (1988); **91,** 7415–7436 (1989).
4. Rosker, M. J., Rose, T. S. & Zewail, A. H. *Chem. Phys. Lett.* **146,** 175 (1988).
5. Atkins, P. W. *Physical Chemistry* 4th edn (Oxford University Press, New York, 1990).
6. Lee, S-Y., Pollard, W. T. & Mathies, R. A. *J. chem. Phys.* **90,** 6146–6150 (1989).
7. Engel, V., Metiu, H., Almeida, R., Marcus, R. A. & Zewail, A. H. *Chem. Phys. Lett.* **152,** 1 (1988).
8. Bernstein, R. B. & Zewail, A. H. *J. chem. Phys.* **90,** 829–842 (1989).
9. Rosker, M. J., Dantus, M. & Zewail, A. H. *Science* **241,** 1200–1202 (1988).
10. Bower, R. D. *et al. J. chem. Phys.* **89,** 4478–4489 (1988).
11. Cong, P., Mokhtari, A. & Zewail, A. H. *Chem. Phys. Lett.* **172,** 109 (1990).
12. Engel, V. & Metiu, H. *J. chem. Phys.* **91,** 1596–1602 (1989).

ACKNOWLEDGEMENTS. This work was supported by the US Air Force.

Large variations in potential vorticity at small spatial scales in the upper ocean

R. T. Pollard* & L. Regier†

* Institute of Oceanographic Sciences, Deacon Laboratory, Brook Road, Wormley, Godalming, Surrey GU8 5UB, UK
† Scripps Institution of Oceanography, A-030, La Jolla, California 92093, USA

THE depth of the ocean's surface layer and stratification of the seasonal thermocline have long been thought to be controlled by heat exchange with the atmosphere and wind-induced mixing. Here we present observations which show that distortion by oceanic eddies also exerts an important influence on the structure of the upper ocean. Eddies induce horizontal shears, which are alternately cyclonic and anticyclonic on scales of 10–20 km. Conservation of potential vorticity then results in vertical motions which modify the stratification of the seasonal thermocline and can change its depth by 100 m or more in a few days. By subducting surface waters and transporting phytoplankton across the seasonal thermocline in a time comparable to that required to double the population, these motions are important to both the physics and the biology of the upper ocean.

One of us[1] has described the density structure of an oceanic front using data from an eight-leg survey in February 1986[2] obtained with a towed conductivity-temperature-depth measurement package (SeaSoar). The separation of isopycnals was very variable and there was a tendency for isopycnals in the thermocline beneath the surface outcrop of the front to deepen, suggestive of downward vertical velocities. We now have absolute velocity profiles from an acoustic Doppler current profiler (ADCP)[3,4], which can resolve similar scales to the SeaSoar (a few metres vertically, a few kilometres horizontally).